MAGNETIC RESONANCE IN CHEMISTRY, VOL. 35, 227–236 (1997)

Structural NMR Studies on Aryl-Substituted π-Allyl–Pd(II) Complexes by Concerted Use of Gradient-Based Experiments

Ramón Malet, Marcial Moreno-Mañas, Francesca Pajuelo, Teodor Parella* and Roser Pleixats
Department of Chemistry, Universitat Autònoma de Barcelona, E-08193 Bellaterra, Barcelona, Spain

Complete ^{1}H and ^{13}C NMR assignments of several aryl-substituted π-allyl–Pd(II) complexes were achieved using modern gradient-based 1D and 2D experiments. In addition, unambiguous ^{31}P assignments were readily made using an improved gradient-enhanced ^{1}H–^{31}P HMBC experiment from which the regiochemistry of cationic complexes containing asymmetric bidentate ligands could also be elucidated. The effect of the nature of the substituent on allylic proton and carbon chemical shifts is briefly evaluated. Finally, a partial π–σ–π isomerization mechanism is proposed taking into account some observed dynamic NMR processes which are largely dependent on the ligand nature of these complexes. © **1997 by John Wiley & Sons, Ltd.**

Magn. Reson. Chem. **35**, 227–236 (1997) No. of Figures: 10 No. of Tables: 4 No. of References: 26

Keywords: NMR; ^{1}H NMR; ^{13}C NMR; ^{31}P NMR; NOE; π-allyl–Pd(II) complexes; gradient-enhanced spectroscopy; ^{1}H–^{31}P correlation

Received 30 April 1996; revised 21 October 1996; accepted 21 October 1996

INTRODUCTION

Linear free energy relationships (LFER) correlating NMR data with Hammett constants constitute a useful technique for determining the transmission of inductive and electronic resonance effects through aryl systems. Thus, we have recently described the preparation and the correlations of chemical shift differences, $\Delta\delta$, with Hammett substituent constants of several η^3-allylic Pd complexes[1–3] and found that such an approach is a good tool for studying the mechanisms of the transmission of electronic effects from the ligands to the allylic moiety and for determining the distribution of the positive charge density in these cationic complexes.

Several efforts have been directed towards studying the three-dimensional solution structure of π-allyl–Pd complexes[4–11] and, specifically, their characteristic dynamic processes.[12–16] We report here the NMR structural analysis of two different types of π-allyl–Pd(II) complexes containing aryl substituents in the allyl moiety. The complete ^{1}H, ^{13}C and ^{31}P assignments were made by the concerted use of several gradient-enhanced experiments such as 2D COSY,[17] ^{1}H–^{13}C 2D HMQC,[18] ^{1}H–^{13}C 2D HMBC[18,19] and ^{1}H–^{31}P 2D HMBC experiments. On the other hand, NOE data were extracted from phase-cycled 2D NOESY spectra[20] or from a gradient-enhanced 1D ROESY (GROESY) experiment[21] when selective excitation on the target proton was possible. From these results, the structure and related dynamic processes have been studied and a partial π–σ–π isomerization mechanism is proposed which is largely dependent on the ligand nature in these complexes.

RESULTS AND DISCUSSION

Bis(μ-chloro)bis[1-(4-X-phenyl)-η^3-allyl]dipalladium (**1**) and bis(μ-chloro)bis[3-phenyl-1-(4-X-phenyl)-η^3-allyl] dipalladium (**2**) complexes (Scheme 1) exhibit simple NMR spectra in which the presence of only the more stable *syn* or *syn–syn* forms of the presumed *trans*

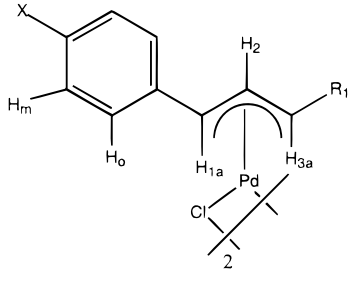

1 R_1=H

2 R_1=Ph

X: (a) NO_2, (b) Br, (c) Cl, (d) H, (e) Me, (f) OMe

Scheme 1

* *Correspondence to*: T. Parella.
Contract grant sponsor: DGICYT; *Contract grant number*: PB90-0063; *Contract grant number*: PB93-0896.
Contract grant sponsor: CICYT; *Contract grant number*: GRQ-2011.

 CCC 0749–1581/97/040227–10 $17.50

isomers, respectively, are observed in solution. Thus, the aryl substituents are always found in a *syn* position with respect to the central proton H-2, and consequently H-1a, H-2 and H-3a protons always represent an *anti–anti* arrangement ($J_{1a2} \approx J_{23a} \approx 11$–$12$ Hz). The H-3a and H-3s protons exhibit minimal mutual coupling (<1 Hz) and aryl *ortho* protons (H_o) are assigned by ROE enhancement obtained from H-1a (and H-3a in **2**) in GROESY spectra. Our results are in agreement with the general observation that the proton resonance frequency of H^{syn} is higher than that of H^{anti}. These dimers can be used as precursors of the cationic complexes **3**–**6**[1–3] (Scheme 2) and their ^{1}H and ^{13}C chemical shifts and *J*(HH) coupling constants are listed in Table 1. As a general trend, we found that the more electron-withdrawing is the substituent X, the more shielded are H-1 and C-1 whereas H-2, H-3, C-2 and C-3 appear to be more deshielded.

On the other hand, we have also studied some mono- and diaryl-substituted Pd(II) tetrafluoroborate com-

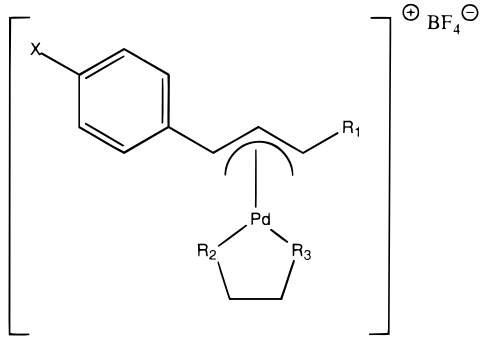

3 R_1=H R_2=R_3=PPh_2

4 R_1=Ph R_2=R_3=PPh_2

5 R_1=H R_2=NMe_2 R_3=PPh_2

6 R_1=H R_2=PPh_2 R_3=NMe_2

X: (a) NO_2, (b) Br, (c) Cl, (d) H, (e) Me, (f) OMe

Scheme 2

plexes (**3**–**6**) containing two different bidentate ligands: (i) 1,2-(diphenylphosphino)ethane and (ii) (1-dimethylamino-2-diphenylphosphino)ethane (Scheme 2). To study how the electronic effects are transmitted from the symmetric or asymmetric bidentate ligand to the allylic system via the palladium atom requires a full signal assignment characterization of such compounds. Table 2 shows the more relevant ^{1}H, ^{13}C and ^{31}P chemical shifts and Table 3 summarizes the most important homo- and heteronuclear coupling values of these complexes.

Allylic proton and carbon assignments in **3** and **4** could also be easily achieved by simple analysis of COSY and HMQC spectra. In general, the influence of the inductive and resonance effects of the substituent on allylic ^{1}H and ^{13}C chemical shifts follows the same trends as observed for **1** and **2**. However, the presence of aryl substituents at both ends of the allylic substructure in **4** complicates the assignment of the aromatic protons. Sometimes, a ^{31}P-decoupled ^{1}H spectrum was useful for simplifying such spectral analysis (Fig. 1).

The crucial step in such assignments was the analysis of NOE data, which revealed through-space interactions between the H-1 and H-3 protons with the corresponding aromatic H_o protons of each aryl ring. In the case of H-1, this H_o proton was correlated in a two-spin AB system (ring A), whereas in the case of H-3, the H_o proton belongs to a AA′BB′C system (ring B) (Table 4). However, phenyl groups bound at the same phosphorus atom in the ligand are not equivalent and, therefore, a complete spectral assignment of aromatic protons was often difficult to achieve because of the presence of a large number of overlapped resonances in a very narrow spectral region. The complete proton assignment of aryl systems was achieved by the concerted use of COSY and NOESY spectra. Among the above-mentioned NOE cross-peaks, weaker but significant inter-ligand NOE enhancements were observed between the H-1a/H-3a protons and the corresponding H_o protons of only one aryl system of the allyl ligand framework (Fig. 2), providing an unequivocal stereochemical assignment of all aryl systems (Table 4).

Another inconvenience arose in the case of **4c** because both H-1 and H-3 had the same chemical shift and,

Table 1. ^{1}H and ^{13}C chemical shifts (ppm) and *J*(HH) coupling constants (Hz) of complexes 1 (in $CDCl_3$)[a] and 2 (in DMSO-d_6)

Compound	H-1	H-2	H-3a	H-3s	H_o	H_m (H_p)	Ring B (*o*/*m*/*p*)[b]	C-1	C-2	C-3	J_{12}	J_{23a}	J_{3a3s}
1a	4.50	5.85	3.16	4.08	7.59	8.10	—	83.16	115.12[a]	66.33	11.3	12.1	6.2
1b	4.52	5.74	3.03	3.97	7.37	7.31	—	85.70	113.63[a]	64.97	11.0	12.1	6.6
1c	4.52	5.73	3.02	3.96	7.38	7.21	—	85.61	113.57[a]	64.86	11.3	12.1	6.9
1d	4.59	5.76	3.00	3.93	7.46	7.20 (7.34)	—	81.70	105.82	59.34	11.3	12.1	6.9
1f	4.64	5.69	2.94	3.88	7.41	6.78	—	82.54	104.42	58.47	11.3	11.7	6.6
2a	5.22	7.12	5.36	—	7.95	8.15	7.75/7.36/7.42	79.50	108.80	85.15	11.0	12.1	—
2c	5.22	6.97	5.22	—	7.74	7.38	7.74/7.38/7.38	82.30	107.77	83.72	11.3	11.3	—
2d	5.25	6.98	5.25	—	7.74	7.40 (7.40)	7.74/7.40/7.40	83.60	107.50	83.60	11.7	11.7	—
2e	5.25	6.91	5.20	—	7.65	7.17	7.74/7.36/7.40	84.34	107.02	83.17	12.4	12.4	—
2f	5.30	6.85	5.13	—	7.70	6.92	7.73/7.35/7.35	85.02	106.06	82.34	12.1	11.7	—
2g[c]	5.22	7.13	5.36	—	8.00	8.19	7.79/7.43	79.97	109.35	83.96	12.1	12.1	—

[a] Except for ^{13}C NMR data for compounds **1a**, **1b** and **1c** (in DMSO-d_6).
[b] Ring B corresponds to the run substituted phenyl ring at position 3 (=R_1) in **2**.
[c] X = NO_2 and R_1 = 4-Cl-Ph.

Table 2. ^{1}H, ^{13}C and ^{31}P chemical shifts (ppm) of complexes 3–6 (in $CDCl_3$)

Compound	H-1a	H-2	H-3a	H-3s	C-1	C-2	C-3	P-1[a]	P-2[a]
3a	5.41	6.44	3.60	4.73	89.84	120.00	69.27	50.44	51.97
3b	5.40	6.22	3.55	4.68	93.09	117.56	67.15	48.57	50.97
3c	5.38	6.23	3.49	4.64	—[b]	—[b]	—[b]	47.46	50.90
3d	5.32	6.27	3.42	4.60	95.20	116.95	66.35	47.14	50.89
3e	5.36	6.20	3.37	4.57	95.83	116.20	65.77	45.93	49.99
3f	5.39	6.16	3.32	4.53	96.66	114.11	65.25	45.95	49.48
4a	5.53	6.77	5.64	—	84.70	113.11	93.95	47.74	50.26
4c	5.50	6.58	5.50	—	88.17	111.78	91.14	46.17	47.70
4d	5.49	6.63	5.49	—	90.10	111.60	90.10	47.09	47.09
4e	5.49	6.53	5.40	—	90.72	111.04	89.54	46.21	46.21
4f	5.51	6.50	5.32	—	91.45	110.32	88.90	46.08	45.49
4g[c]	5.43	6.82	5.55	—	85.41	113.75	91.84	47.62	48.82
5a	5.54	6.42	3.47[d]	3.47[d]	96.08	117.01	51.23	41.77	—
5b	5.48	6.16	3.42	4.09	99.32	114.49	50.48	40.04	—
5d	5.46	6.17	2.99	3.81	100.48	113.91	49.89	39.98	—
5e	5.45	6.10	2.99	3.37	101.29	113.04	49.41	40.26	—
5f	5.51	6.07	2.93	3.81	101.95	111.97	48.94	38.70	—
6a	4.83	6.45	4.27	4.83	69.65	120.68	80.96	—	39.25
6b	4.74	6.28	4.09	4.68	—[b]	—[b]	—[b]	—	36.39
6d	4.74	6.28	4.05	4.65	—[b]	—[b]	—[b]	—	35.33
6e	4.80	—[b]	—[b]	4.62	—[b]	—[b]	—[b]	—	—[b]
6f	4.85	6.25	3.97	4.59	—[b]	—[b]	—[b]	—	33.98

[a] P1 and P2 correspond to phosphorus atoms placed *trans* and *cis*, respectively, with respect to H-1.
[b] Not measured.
[c] X = NO_2 and R_1 = 4-Cl-Ph.
[d] Signals appearing as a simple broad resonance.

therefore, the NOE data gave ambiguous answers. In this case, the cross peak signals appearing in the ^{1}H–^{13}C HMBC spectra between the previously assigned H_o protons of each aryl ring in the allyl system and the C-1 or C-3 carbons allowed unambiguous ^{13}C and ^{31}P assignments to be made.

Unambiguous ^{31}P resonance assignments were usually achieved by using long-range proton–

Table 3. *J*(HH), *J*(HP), *J*(CP) and *J*(PP) coupling constants (Hz) of complexes 3–6

Compound	H1a–H2	H2–H3a	H2–H3s	H1a–P1	H3a–P2	H3s–P2	C1–P1	C1–P2	C2–P1	C2–P2	C3–P1	C3–P2	P1–P2
3a	—[a]	—[a]	—[a]	11.2	—[a]	—[a]	27.7	6.5	6.5	6.5	5.0	25.5	42.5
3b	—[a]	—[a]	—[a]	—[a]	—[a]	—[a]	26.5	6.6	6.6	6.6	5.2	24.6	40.7
3c	13.5	13.5	8.0	11.3	12.2	6.8	—[b]	—[b]	—[b]	—[b]	—[b]	—[b]	41.2
3d	13.5	13.3	7.7	11.6	12.8	6.8	26.8	6.5	6.9	6.9	6.5	26.8	41.5
3e	13.3	13.3	7.4	12.2	12.1	6.9	25.9	6.5	6.5	6.5	4.6	27.7	40.7
3f	13.2	13.2	7.7	11.2	11.5	6.9	25.9	6.5	6.9	6.9	4.6	27.7	40.7
5a	13.2	13.2	9.7	9.1	—	—	27.7	—	—[a]	—	4.6	—	—
5b	13.5	13.0	9.5	9.1	—	—	25.7	—	—[a]	—	—[a]	—	—
5d	13.4	12.9	9.9	9.2	—	—	25.9	—	5.5	—	3.7	—	—
5e	13.5	—[a]	—[a]	9.1	—	—	25.9	—	5.5	—	2.8	—	—
5f	13.5	12.1	7.4	8.8	—	—	24.9	—	5.5	—	2.8	—	—
6a	—[a]	13.7	—[a]	—	9.2	—[a]	—	5.5	—	5.6	—	24.8	—
6b	11.6	—[a]	7.6	—	7.5	6.3	—	—[b]	—	—[b]	—	—[b]	—
6d	12.3	13.1	6.6	—	9.8	3.3	—	—[b]	—	—[b]	—	—[b]	—
6e	12.0	—[a]	—[a]	—	—[a]	—[a]	—	—[b]	—	—[b]	—	—[b]	—
6f	12.5	—[a]	7.4	—	9.2	7.4	—	—[b]	—	—[b]	—	—[b]	—
4a	12.7	12.7	—	13.2	10.1	—	25.9	6.5	7.4	7.4	6.5	24.1	50.4
4c	12.6	12.6	—	—[a]	—[a]	—	26.8	6.5	7.4	7.4	6.5	24.1	48.6
4d	12.8	12.8	—	—[a]	—[a]	—	15.7	15.7	7.4	7.4	15.7	15.7	—[c]
4e	13.0	12.8	—	—[a]	—[a]	—	15.7	15.7	7.4	7.4	15.7	15.7	—[c]
4f	13.0	12.8	—	9.3	9.9	—	22.2	8.3	7.4	7.4	9.2	23.1	48.3
4g[d]	12.8	12.8	—	7.9	9.9	—	25.0	7.4	6.5	6.5	7.4	23.1	50.6

[a] Not measured owing to line broadening or overlapped signals.
[b] Not detected.
[c] The ^{31}P spectrum showed only a single resonance.
[d] X = NO_2 and R_1 = 4-Cl-Ph.
[e] The corresponding H3a–H3s, H1a–P2, H2–P1, H2–P2, H3a–P1 and H3s–P1 couplings were unresolved. However, the H1–P2 and H3–P1 couplings in complexes **6** were sometimes resolved, showing a value in the range 2.6–3.3 Hz.

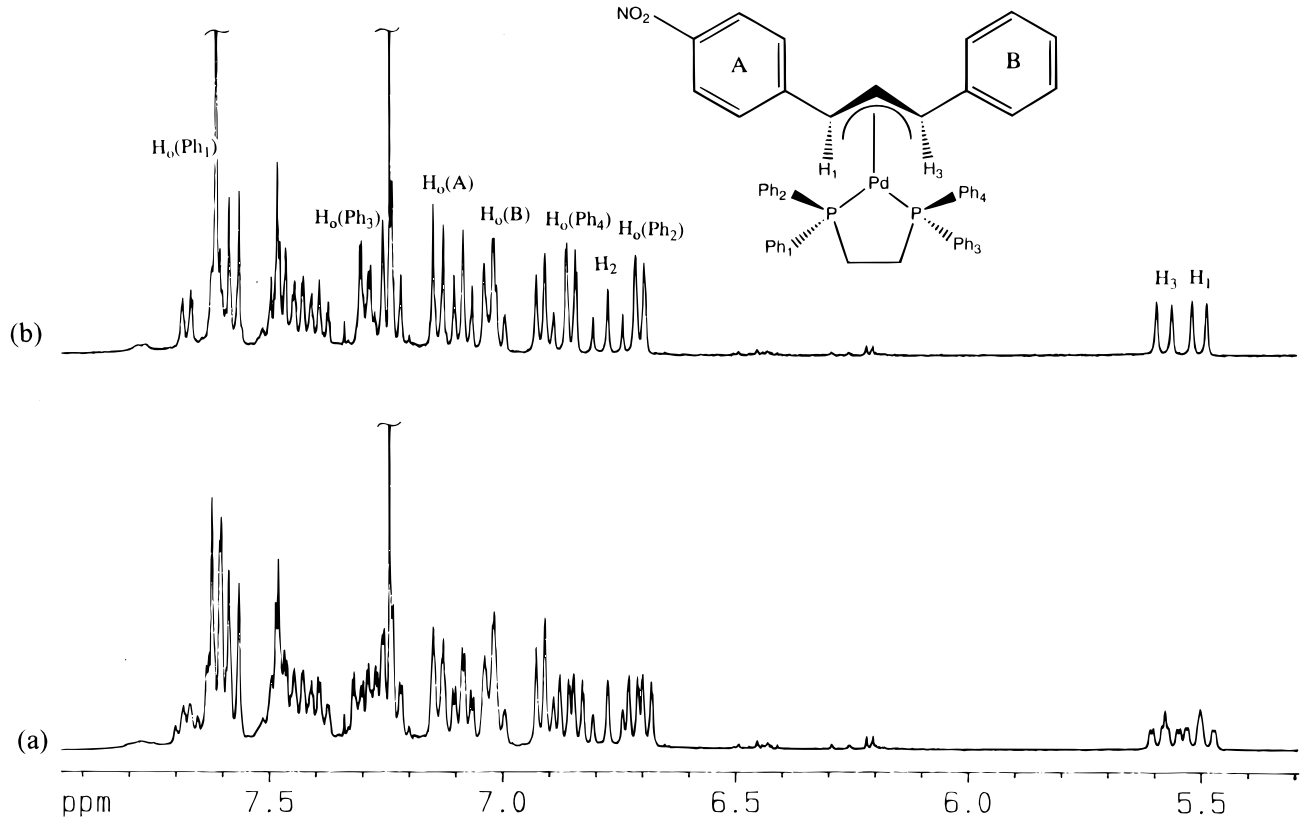

Figure 1. Expanded aromatic and olefinic section of the (a) conventional 400 MHz ^{1}H spectrum and (b) broadband ^{31}P-decoupled ^{1}H spectrum of **4a**. The signals assigned to the allylic and aryl *ortho* protons are labelled.

phosphorus ($^{n}J_{HP}$, $n > 1$) and carbon–phosphorus ($^{n}J_{CP}$, $n > 1$) coupling constants because in pseudo-planar complexes the *trans* coupling values are generally larger than the corresponding *cis* coupling values. A simple way to deduce ^{1}H–^{31}P connectivities is from a selective ^{31}P-decoupled proton spectrum, although a more general approach for this purpose would be a 2D ^{1}H–^{31}P long-range correlation experiment.[22,23] We used a single-scan 2D ^{1}H–^{31}P HMBC experiment (Fig. 3) in which the desired coherence selection is achieved

Table 4. Aromatic ^{1}H chemical shifts (ppm) of complexes 4, 5a and 6a (in $CDCl_3$)

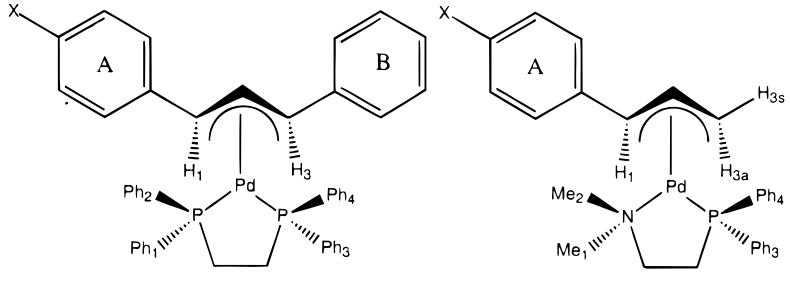

4 **5**

Compound	Ph_A ortho	Ph_A meta	Ph_A para	Ph_B ortho	Ph_B meta	Ph_B para	Ph_1 ortho	Ph_1 meta	Ph_1 para	Ph_2 ortho	Ph_2 meta	Ph_2 para	Ph_3 ortho	Ph_3 meta	Ph_3 para	Ph_4 ortho	Ph_4 meta	Ph_4 para
4a	7.13	7.57	—	7.02	6.90	7.01	7.62	7.62	7.68	6.70	7.08	7.24	7.30	7.48	7.43	6.85	7.23	7.39
4b	6.96	6.83	—	7.05	6.95	7.02	7.60	—[a]	—[a]	6.79	7.19	7.37	7.39	—[a]	—[a]	6.73	7.17	7.37
4e	6.90	6.71	—	6.98	6.92	7.00	7.47	—[a]	—[a]	6.74	7.15	7.33	7.38	—[a]	—[a]	6.74	7.11	7.33
4f	6.95	6.44	—	7.00	6.90	7.00	7.45	—[a]	—[a]	6.76	7.14	7.33	7.37	—[a]	—[a]	6.76	7.14	7.33
4g	7.11	7.57	—	6.95	6.77	—	7.52	7.58	—[a]	6.74	7.12	7.28	7.37	—[a]	—[a]	6.82	7.24	7.40
5a	7.83	8.20	—	—	—	—	—	—	—	—	—	—	7.61	7.65	7.52	7.61	7.65	7.52
6a	7.13	7.54	—	—	—	—	7.64	—[a]	—[a]	6.83	7.10	7.26	—	—	—	—	—	—

[a] Overlapped resonances appearing in the range 7.45–7.65 ppm.

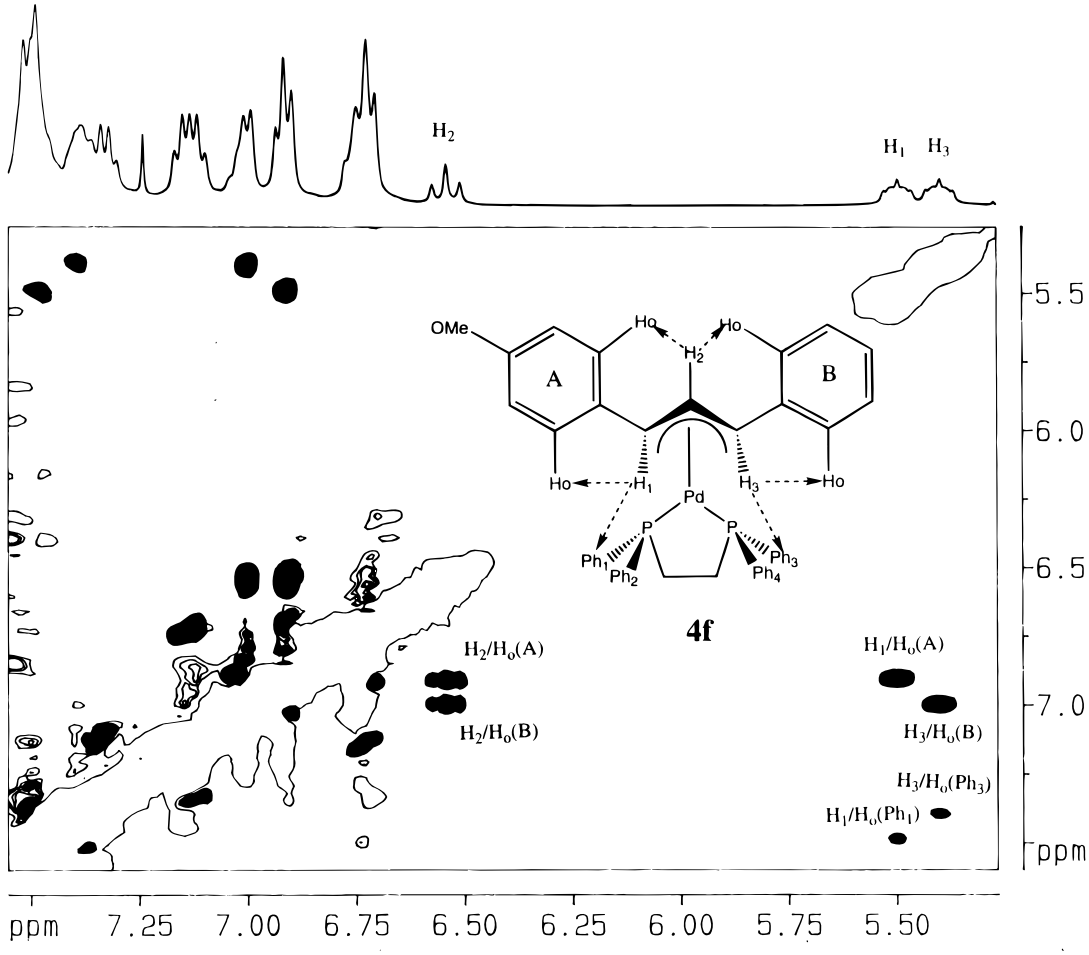

Figure 2. Phase-sensitive 2D NOESY spectrum of **4f** recorded with a mixing time of 500 ms. Black-filled cross-peaks stands for a negative NOE correlation.

by means of PFG (similar results can be obtained by introducing coherence rejection in a gradient-based long-range optimized HSQC pulse train, as described recently[24]). In this way, a clean 2D ^{1}H–^{31}P map showing all two- and three-bond proton–phosphorus connectivities is quickly obtained in a few minutes without the need for a complete phase cycle. Gradient

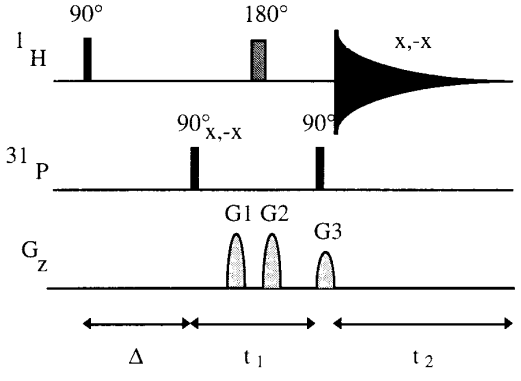

Figure 3. Pulse sequence for recording gradient-enhanced single-scan ^{1}H–^{31}P HMBC spectra. Δ is optimized to $1/2J_{HP}$ and the gradient ratio is 1.238:1.238:1. All pulses are applied along the *x*-axis. A minimum two-step phase cycle in which the first 90° (^{31}P) pulse and the receiver are inverted on alternate scans can be applied in order to remove possible axial peaks appearing at $F_1 = 0$.

ratios must be optimized according to the proton and phosphorus gyromagnetic ratios. The general condition for optimal N-type signal rephasing is as follows:

$$(\gamma_H + \gamma_P)G_1 - (\gamma_H - \gamma_P)G_2 - \gamma_H G_3 = 0 \qquad (1)$$

Thus, taking in account that $\gamma_H/\gamma_P \approx 2.47$, a 1.238:1.238:1 gradient ratio affords one possible solution.

In the resulting ^{1}H–^{31}P HMBC spectra we only observe clear cross peaks between the allylic proton and the phosphorus atom placed in a *trans* arrangement among other intra-ligand interactions. On the other hand, cross peaks arising from *cis* connectivities or from the central allylic H-2 protons were usually missing because $J < 2.5$ Hz (Fig. 4).

Complexes **5** (*trans*) and **6** (*cis*) exist as an equilibrium mixture where the *trans* isomers **5** were always shown to be the major compounds, as deduced from the ^{1}H–^{31}P HMBC spectra (Fig. 5) and NOE data (Figs 6 and 7). The ^{1}H-decoupled ^{31}P spectra revealed two singlets where the signal ratios could be easily analysed and integrated. The *cis* percentage in the mixture increased with increasing electron-withdrawing character of the substituent on the aryl ring. However, except in the nitro derivative, the quantity of *cis* isomer **6** was always small and this fact, together with solubility limitations, prevented some NMR parameters from being

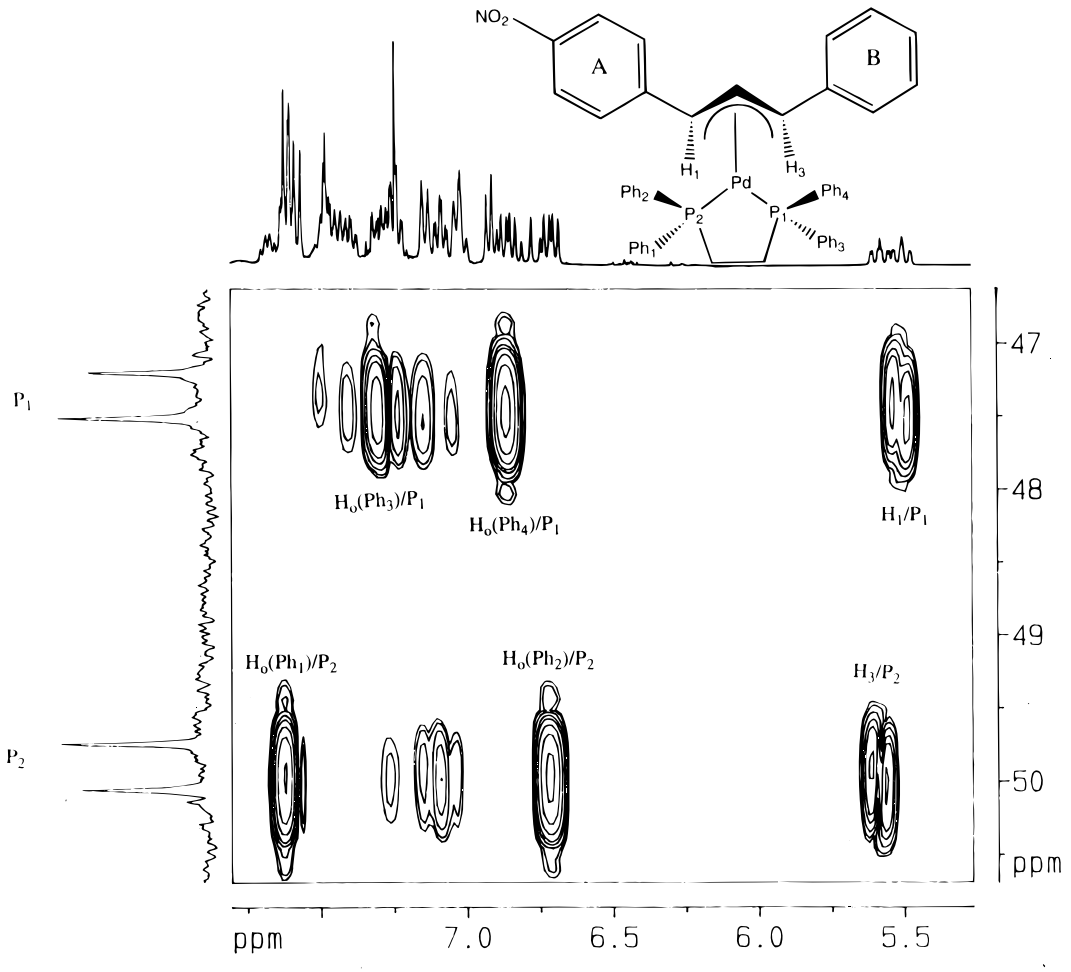

Figure 4. ^{1}H–^{31}P HMBC spectrum of **4a**.

determined. In contrast to **3** and **4**, some dynamic processes were observed in both ligand and allyl moieties in complexes **5** in which line broadening and/or coalescence of the H-3a/H-3s protons and the two different NMe resonances were observed.

For instance, the GROESY spectrum of **5f** after selectively pulsing on the methyl singlet resonating at δ 2.01 (Fig. 6) showed clean ROE enhancement in the methylene protons of the ligand (δ 2.74) and inter-ligand ROE to H-1a, H_o and H_m protons of the allyl framework, confirming the stereochemistry. On the other hand, a strong negative signal was also observed for the other NMe resonance (δ 2.58) due to saturation transfer by exchange chemical processes. Similar results could be observed from the analysis of 2D NOESY spectra (Fig. 7). Crucial negative cross peaks arising from inter-ligand cross relaxation are observed for the H_o/NMe pairs, stronger positive cross peaks due to exchange processes between H-3a/H-3s and the two NMe signals, and false NOE cross peaks were therefore observed for the other H_o/NMe pair and the H-3a/H-2 and H-1/H-3s pairs. All these data confirm the relatively short distance between the ligand and the allylic frameworks. The stereochemistry of these compounds was confirmed from the ^{1}H–^{31}P HMBC spectra (Fig. 5), in which the H-1a resonance in the major isomer **5a** showed a strong cross peak with the major ^{31}P resonance, whereas both H-3a and H-3s protons in the minor isomer showed cross peaks with the minor ^{31}P resonance. In addition, evidence for the equivalence of the two phenyl groups in the ligand moiety in compounds **5** could also be deduced from these spectra. Thus, the major ^{31}P resonance only showed a single strong correlation to aryl H_o protons (δ 7.61) whereas the minor signal corresponding to isomer **6** showed two different correlations on the aryl protons resonating at δ 7.64 and δ 6.83 (Table 4).

It is also important to describe the influence of the nature of the ligand on the chemical shifts of the allylic moiety (Tables 2 and 4). Thus, H-3s and C-3 resonances in **5** and H-1a, H_o (ring A), H_m (ring A) and C-1 resonances (not established for all compounds) in **6** are shielded up to 0.8 ppm when compared with complexes **3**, basically owing to the donor character of the nitrogen atom. On the other hand, a minor deshielding effect is observed for H-1a and C-1 in **5** and H-3a and C-3 in **6** when compared with **3**.

In summary, from the experimental dynamic processes observed in **5**, we think that a π–σ–π (also called η^3–η^1–η^3) isomerization mechanism mainly operates in these complexes **5** containing an non-symmetric ligand (Scheme 3). Thus, a fast η^3–η^1 isomerization in the *trans* isomer takes place in which the C-3 carbon becomes an sp^3 carbon. Subsequently, a fast rotation around the C-2—C-3 σ-bond followed by a fast recoordination of the olefin would explain the exchange between H-3a/H-3s protons and between the two equivalent NMe and

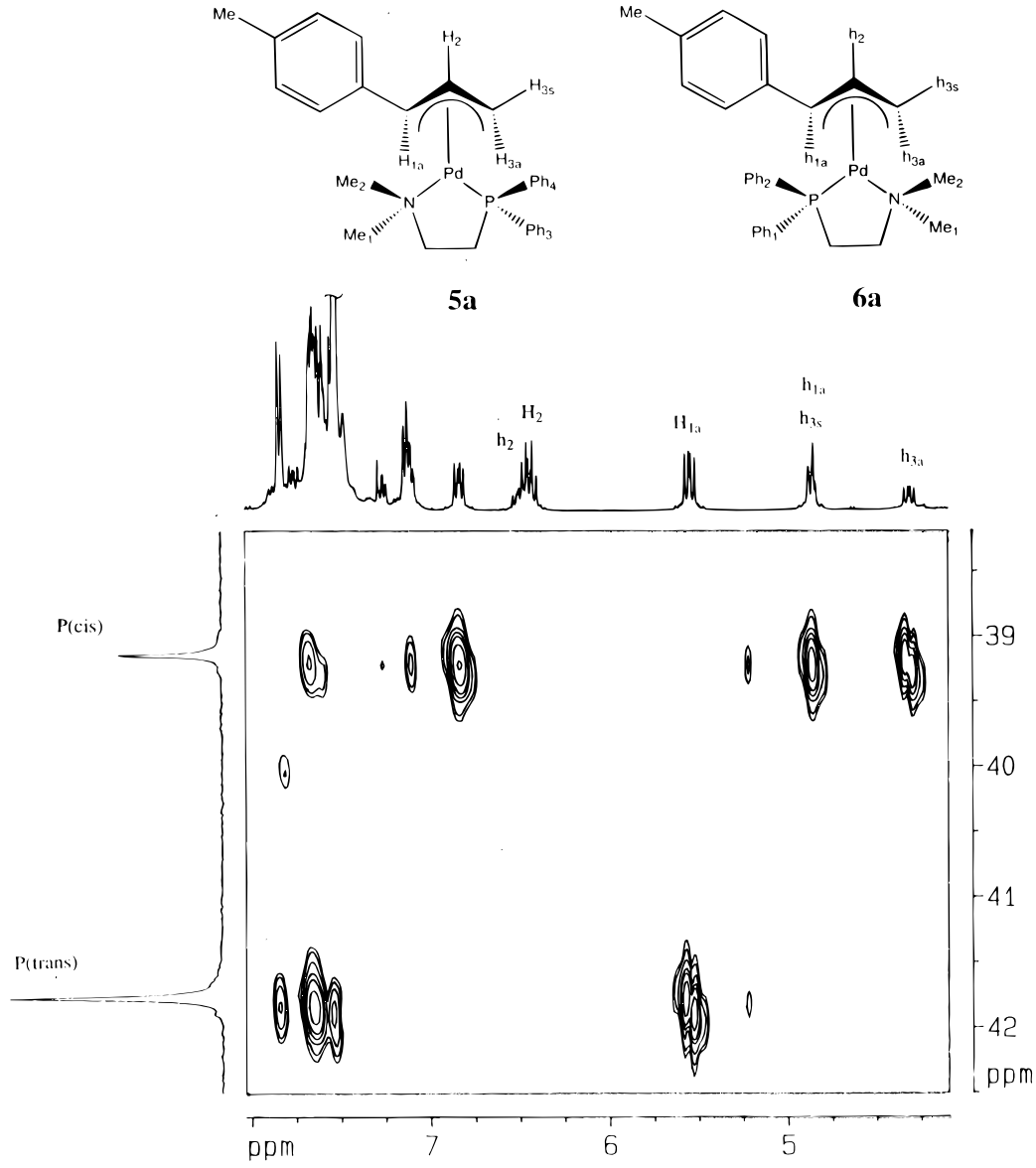

Figure 5. ^{1}H–^{31}P HMBC spectrum of **5a** + **6a**. Allylic protons of the major isomer are labelled with upper-case letters and those of the minor isomer with lower-case letters.

PPh groups, respectively. On the other hand, this isomerization mechanism is not present for the *cis* isomer **6**, because no exchange process between any pair of *syn–anti* and ligand signal was observed. For instance, all H-3 and NMe protons in these complexes **6** always present sharp resonances in the conventional ^{1}H spectrum for which no positive cross peaks due to exchange are observed in the corresponding NOE spectra. In addition, there is no evidence for a dynamic *cis–trans* equilibrium because of the absence of exchange cross peaks between them. On the other hand, since no exchange processes are observed for all complexes **3** and **4**, it may be concluded that in those complexes containing symmetrical ligands any dynamic process also remains slow on the NMR time-scale. In summary, from the NMR data presented only a π–σ–π isomerization mechanism can be proposed for complexes **5** and no experimental evidence for an apparent Pd–allyl rotation[25] has been observed.

EXPERIMENTAL

All experiments were performed on a Bruker ARX400 spectrometer equipped with an inverse broadband probehead incorporating a shielded Z-gradient coil. Proton and carbon chemical shifts were referenced to the $CDCl_3$ (7.24 and 77.0 ppm, respectively) or DMSO (2.49 and 39.5 ppm, respectively) signals. Phosphorus chemical shifts were referenced to internal phosphoric acid capillary. The general experimental conditions for recording all NMR experiments were as described in the original reports. The number of scans in each experiment was dependent on the sample concentration and the pre-scan delay was always set to 1 s.

ge-2D COSY spectra resulted from a 512 × 1024 data matrix size using a 1:1 gradient combination.[17] The ge-2D ^{1}H–^{13}C correlation (HMQC) spectra resulted

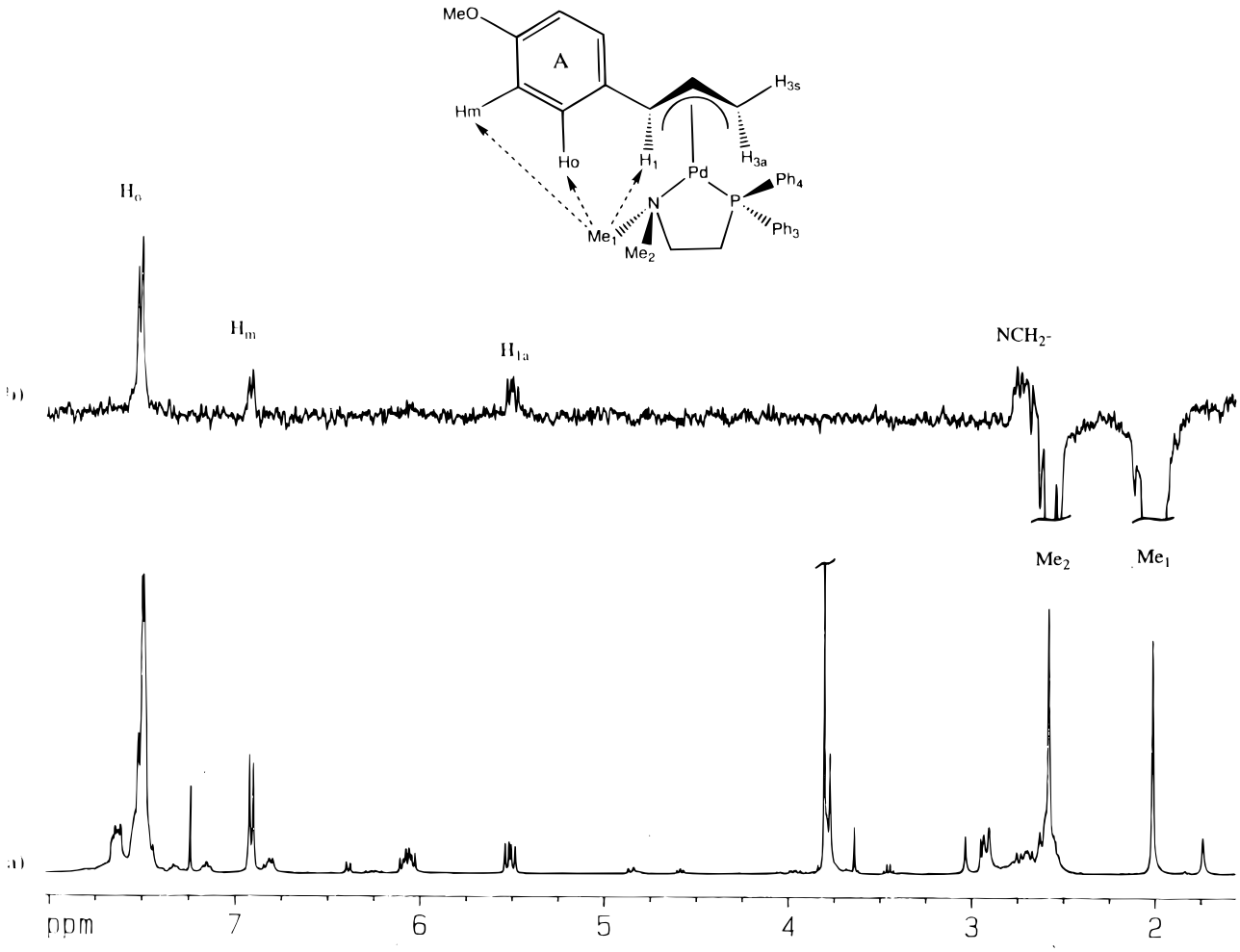

Figure 6. GROESY spectrum of **5f** after selectively pulsing the methyl resonance Me_1. The mixing time was 500 ms.

from a 128 × 1024 data matrix size with two scans per t_1 value using an inter-pulse delay of 3.5 ms and a 2:2:1 gradient combination.[18] The ge-2D ^1H–^{13}C HMBC spectra were acquired using a purged TANGO scheme as a preparation period, an inter-pulse delay of 60 ms and the same gradient ratio as described above for HMQC experiments.[19] In this way, direct responses were efficiently removed and smaller gradient strengths were needed to suppress undesired ^1H–^{12}C magnetization efficiently. ge-2D multiple bond ^1H–^{31}P shift correlation (HMBC) spectra resulted from a 64 × 512 data matrix size using the pulse sequence in Fig. 1.[18] The delay Δ was set to 50 ms and a gradient combination of 1.238:1.238:1 was used to select the desired coherence. The phase-sensitive NOESY experiment resulted from a 2 × 512 × 1024 data matrix size using a mixing time of 500 ms.[20] Quadrature detection in the t_1 dimension was achieved by the TPPI method. High-quality 1D GROESY spectra were obtained with a recently proposed pulse sequence[21] using a 500 ms T-ROESY mixing time.[26] Gaussian pulses of 20 and 40 ms were used as selective 90° and 180° pulses, respectively, and a 1: − 1:2 gradient combination afforded the desired coherence selection. All 2D data were zero-filled once in the t_1 dimension and a sine-bell filter (cosine in NOESY spectra) was used before Fourier transformation in both dimensions. All B_0 field gradient pulses (maximum strength of 15 G cm^{-1}) had a Gaussian shape truncated at 5% and a length of 1 ms followed by a 100 μs recovery delay.

Acknowledgements

Financial support from the DGICYT (Ministry of Education and Science of Spain) through projects PB90-0063 and PB93-0896 and a predoctoral scholarship (R.M.) and from CICYT (Generalitat de Catalunya) through project GRQ-2011 and a predoctoral scholarship (F.P.) are gratefully acknowledged. We also thank the Servei de Ressonància Magnètica Nuclear, UAB, for allocating instrument time to this project.

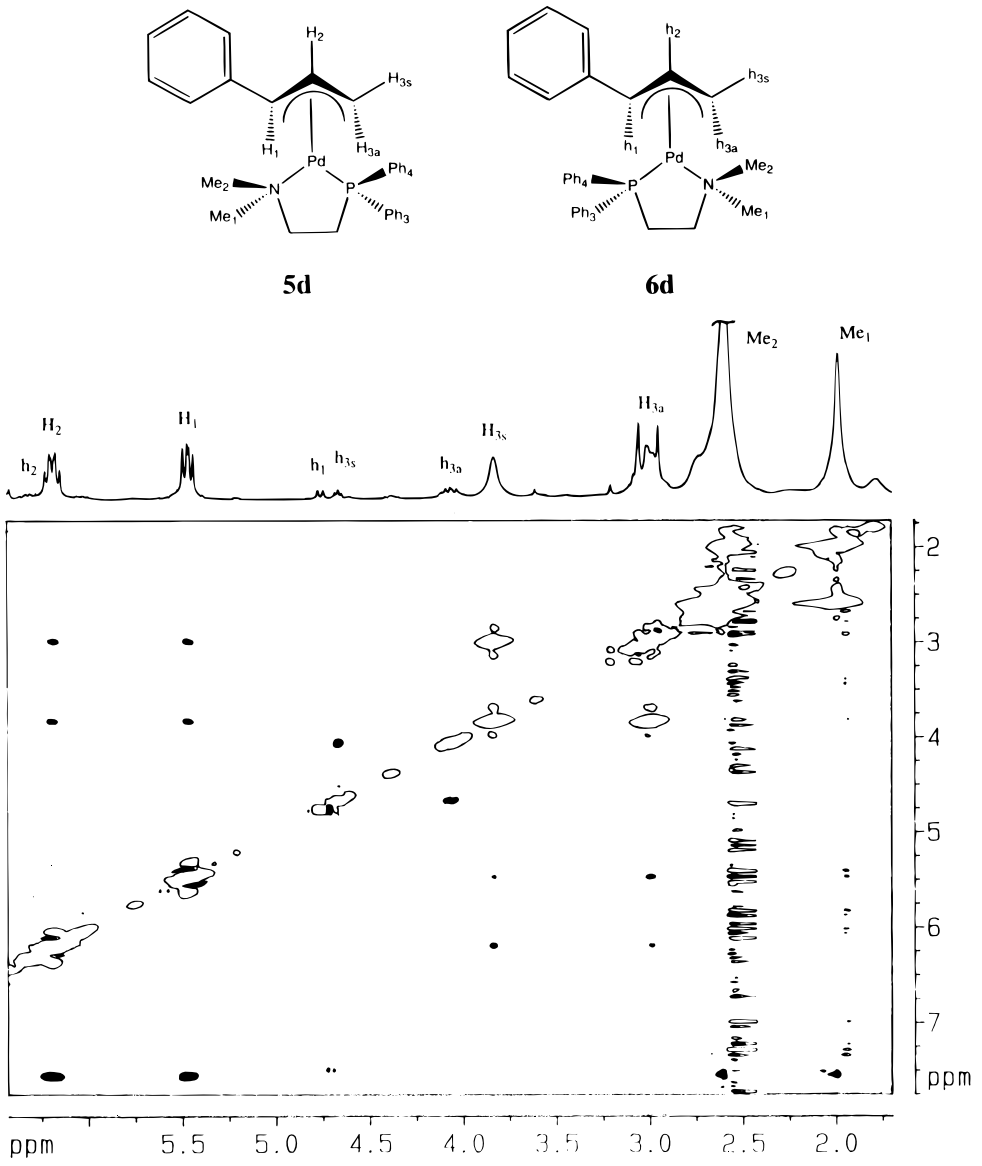

Figure 7. Phase-sensitive NOESY spectrum of **5d** + **6d** recorded with a mixing time of 500 ms. Black-filled cross-peaks stands for a negative NOE correlation whereas positive signals due to exchange processes are shown by unfilled cross peaks.

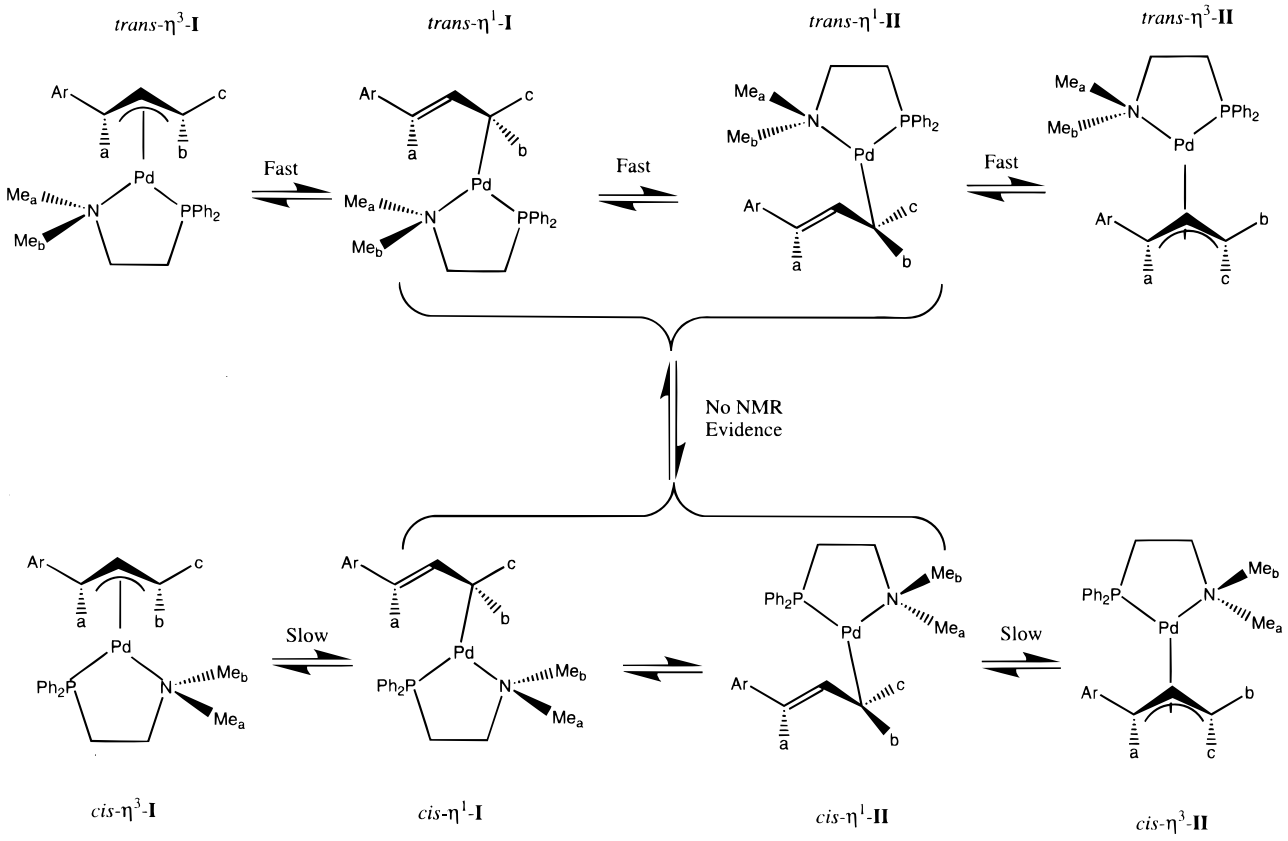

Scheme 3

REFERENCES

1. R. Malet, M. Moreno-Mañas, T. Parella and R. Pleixats, *Organometallics* **14**, 2463 (1995).
2. R. Malet, M. Moreno-Mañas, T. Parella and R. Pleixats, *J. Org. Chem.* **61**, 758 (1996).
3. M. Moreno-Mañas, F. Pajuelo, T. Parella and R. Pleixats, *Organometallics* in press.
4. H. Kurosawa and N. Asada, *Organometallics* **2**, 251 (1983).
5. B. Akermark, B. Krakenberger, S. Hansson and A. Vitagliano, *Organometallics* **6**, 620 (1987).
6. H. Rüegger, R. W. Kunz, Ch. J. Ammann and P. S. Pregosin, *Magn. Reson. Chem.* **29**, 197 (1992).
7. A. Albinati, Ch. J. Ammann, P. S. Pregosin and H. Rüegger, *Organometallics* **9**, 1826 (1990).
8. K. Ohkita, H. Kurosawa, T. Hasegawa, T. Hirao and I. Ikeda, *Organometallics* **12**, 3211 (1993).
9. P. S. Pregosin and R. Salzmann, *Magn. Reson. Chem.* **32**, 128 (1994).
10. P. Barbaro, P. S. Pregosin, R. Salzmann, A. Albinati and R. W. Kunz, *Organometallics* **14**, 5160 (1995).
11. A. Togni, U. Burckhardt, V. Gramlich, P. S. Pregosin and R. Salzmann, *J. Am. Chem. Soc.* **118**, 1031 (1996).
12. P. S. Pregosin and H. Rüegger, *Magn. Reson. Chem.* **32**, 297 (1994).
13. A. Albinati, R. W. Kunz, Ch. Ammann and P. S. Pregosin, *Organometallics* **10**, 1800 (1991).
14. S. Hansson, P. O. Norrby, M. P. T. Sjögren, B. Akermark, M. E. Cucciolito, F. Giordano and A. Vitagliano, *Organometallics* **12**, 4940 (1993).
15. J. Herrmann, P. S. Pregosin, R. Salzmann and A. Albinati, *Organometallics* **14**, 3311 (1995).
16. C. Breutel, P. S. Pregosin, R. Salzmann and A. Togni, *J. Am. Chem. Soc.* **116**, 4067 (1994).
17. R. E. Hurd, *J. Magn. Reson.* **87**, 422 (1990).
18. R. E. Hurd and B. K. John, *J. Magn. Reson.* **91**, 648 (1991).
19. T. Parella, F. Sánchez-Ferrando and A. Virgili, *J. Magn. Reson. A* **112**, 241 (1995).
20. J. Jeener, P. Bachmann and R. R. Ernst, *J. Chem. Phys.* **71**, 4545 (1979).
21. P. Adell, T. Parella, F. Sánchez-Ferrando and A. Virgili, *J. Magn Reson. B* **108**, 77 (1995).
22. V. Sklenar, H. Miyashiro, G. Zon, H. T. Miles and A. Bax, *FEBS Lett.* **208**, 94 (1986).
23. K. V. R. Chary, V. K. Rastogi and G. Govil, *J. Magn. Reson. B* **102**, 81 (1993).
24. M. A. Keniry, *Magn. Reson. Chem.* **34**, 33 (1996).
25. A. Gogoll, J. Örnebro, H. Grennberg and J. E. Bäckvall, *J. Am. Chem. Soc.* **116**, 3631 (1994).
26. T. L. Hwang and A. J. Shaka, *J. Am. Chem. Soc.* **114**, 3157 (1992).

